Ionics (2013) 19:1027–1036
DOI 10.1007/s11581-012-0818-5

ORIGINAL PAPER

Preparation and characterization of zirconium sulfophenyl phosphate-doped sulfonated poly(phthalazinone ether sulfone) composite proton exchange membrane

Suwen Wang · Lei Jin · Zhongfang Li

Received: 21 May 2012 / Revised: 24 September 2012 / Accepted: 14 October 2012 / Published online: 8 November 2012

Abstract Polymer composite membranes based on sulfonated poly(phthalazinone ether sulfone) (SPPES) and zirconium sulfophenyl phosphate (ZrSPP) were prepared. Three ZrSPP concentrations were used: 10, 20, and 30 wt%. The membranes were characterized by infrared spectroscopy (IR), X-ray diffraction spectroscopy, thermal gravimetric analysis, and scanning electron microscopy (SEM). The IR results indicated the formation of intense hydrogen bonds between ZrSPP and SPPES molecules. The SEM micrographs showed that ZrSPP well dispersed with SPPES and form a lattice structure. The proton conductivity of the SPPES (degree of sulfonation (DS) 64 %)/ZrSPP (10 wt%) composite membrane reached 0.39 S/cm at 120 °C 100 % relative humidity and that of the 30 wt% of SPPES (DS 16.1 %)/ZrSPP composite membrane reached 0.18 S/cm at 150 °C. The methanol permeabilities of the SPPES/ZrSPP composite membranes were in the range of 2.1×10^{-8} to $0.13\times10^{-8}\,\mathrm{cm^2/s}$, much lower than that of Nafion®117 ($10^{-6}\,\mathrm{cm^2/s}$). The composite membranes exhibited good thermal stabilities, proton conductivities, and good methanol resistance properties.

Keywords Composite · Proton exchange membrane · Sulfonated poly(phthalazinone ether sulfone) · Zirconium sulfophenyl phosphate

Introduction

Direct methanol membrane fuel cells (DMFCs) have attracted substantial research attention due to their high theoretical energy densities and nontoxicity to the environment [1–3]. Proton exchange membranes are the key components of DMFCs. At present, the commercial perfluorinated membrane such as Nafion is one of the most advanced available membranes for direct methanol fuel cells for its excellent chemical, mechanical, and electrochemical properties as well as high proton conductivity at ambient temperature and high humidity condition [4, 5].

The key technological issues with regards to DMFCs are mostly the low catalytic activity and the high methanol crossover problems [6–8]. The high methanol crossover from anode to cathode is a major problem since it not only causes a loss of fuel (ca. 40 % methanol loss) but also generates mixed potential at oxygen cathode, leading to the poisoning of the catalyst. With the increase of cathodic polarization, battery performance will be degraded obviously. An effective way of solving these issues is to improve the operating temperature of the fuel cells. Increase operating temperatures can improve catalyst efficiency, reduce catalyst poisoning owing to adsorption of CO [9], enhance methanol oxidation rates, and reduce the opportunity to methanol permeability [10, 11]. Proton exchange membrane (PEM) can arise only from 100 to 180 °C. At this temperature, other materials are still available except for conventional Nafion membrane. So fabricating high temperature proton exchange membrane becomes an important research. Many studies have been reported in literature. Among them, nanocomposite membranes by embedding nanosized materials into polymers showed much lower methanol permeability with similar or even improved proton conductivities at high temperature [12]. Even some sulfonated heat-resistant resins composite membranes exhibit good properties than traditional expensive Nafion membranes.

To prepare high temperature membrane, materials must have excellent thermal stability. Poly(phthalazinones) (PPs), include poly(phthalazinone ether sulfone) (PPES) [13], poly

---

S. Wang · L. Jin · Z. Li (✉)
School of Chemical Engineering,
Shandong University of Technology,
12# Zhangzhou Road,
Zibo City, Shandong Province 255049, People's Republic of China
e-mail: lizhf@eyou.com

(phthalazinone ether ketone) [14] are distinguished for their good thermal stability with very high glass transition temperature, chemical stability, and mechanical strength.

We prepared PEM based on sulfonated poly(phthalazinone ether sulfone ketone) (SPPESK) in our previous work [15], but SPPESK membranes' mechanical property and dimension stability in wet/dry is not satisfied. Then, we used porous polytetrafluoroethylene (PTFE) membranes as support material prepared SPPESK/zirconium sulfophenyl phosphate (ZrSPP)/PTFE composite membranes [16]. These SPPESK/ZrSPP/PTFE composite membranes have good mechanical property compared with unsupported SPPESK/ZrSPP membranes. Dimensional stability is also maintained in alternating wet/dry environments. And now, we find PPES has several advantages such as inexpensive, easy sulfonated, and good proton conductivity after sulfonation (SPPES) [17]. SPPES has better solubility and easy simple film fabrication. SPPES proton exchange membranes exhibit good membrane mechanical strength and good dimensional stability of membranes in wet/dry condition. More importantly, it has high proton conductivity and low methanol permeability. SPPES should be an alternative material to Nafion.

Blending membranes with conductive materials is a simple and effective method to fabricate a composite membrane with excellent proton conductivity, enhanced dimensional stability and mechanical properties [18]. Types of clays [19, 20], hygroscopic oxides [21–23], zeolites [24], conductive polymers [25], and heteropolyacid (HPA) [26] have been used in the fabrication of composite membranes. Clays, zeolites, and hygroscopic oxides can increase the water uptake of membranes; there have been no proton conductance capacity. HPA increase both water uptake and concentration of acid sites. However, HPA tends to be lost by dissolution in water. Inorgano–organic materials, such as zirconium sulfoarylphosphonate, $M(HPO_4)_x(O_3PC_6H_4SO_3H)_{2-x}$ and $M(HPO_4)x(O_3P\text{-}R\text{-}NH_2)_{2-x}$ (M=Ti, Zr, Th), have also been reported as excellent additives [17, 19]. The compound $Zr(HPO_4)_{0.65}(SPP)_{1.35}$ is used for doping in SPPEEK. A threefold increase in proton conductivity at 70 °C was observed for a composite membrane with 50 wt% of solid proton conductor under 100 % relative humidity (RH) [27].

ZrSPP, an inorganic–organic proton conductor, is stable up to 200 °C. It also has good conductivity. ZrSPP can form a three-dimension solid-lattice structure. ZrSPP should be a promising filler for composite proton exchange membrane. In the current study, a series of SPPES/ZrSPP composite membranes were synthesized in different sulfonation degree of SPPES and different doping levels of ZrSPP particles by solution casting. The proton conductivity, thermal stabilities, and methanol permeability were tested.

Experimental

Materials and chemicals

Poly(phthalazinone ether sulfone) (PPES) (Dalian Polymer New Material Co., Ltd. WM 452), fuming sulphuric acid (50 % SO_3), *N*,*N*-dimethylacetamide (DMAc), methanol, and sodium hydroxide used were all of analytical grade. SPPES was synthesized using the method described in the literature [17]. ZrSPP was obtained following also the procedure described in the literature [15].

Preparation of the SPPES/ZrSPP composite membranes

A higher DS of SPPES can lead to higher proton conductivity. However, an increase in DS also indicates detrimental effects to the mechanical properties and thermal endurance of PEM membranes due to the hydrophilicity of the sulfonic acid groups. SPPES samples with appropriate DS were selected for this reason.

A series of SPPES/ZrSPP composite membranes was prepared by solution cast method. SPPES was dissolved in DMAc and stirred for 10 h at room temperature. Then, the solution was filtered. For the composite membranes, proportional amounts of ZrSPP were added to the solution to obtain wt% of 10, 20, and 30 %. The homogenous solution was cast onto a glass plate and dried at 70 °C for 24 h. The membranes were immersed in 1 mol/L H_2SO_4 and then washed with deionised water.

Scanning electron microscopy and energy dispersive X-ray spectroscopy

The morphology of the membranes was investigated using a scanning electron microscope (FEI Sirion 200). To view the cross-section of the membranes, all the samples were fractured after being soaked in cryogenic conditions. And the fresh cross-section was imaged after a thin layer of gold was vacuum-sputtered onto it. Elemental distribution of ZrSPP in composite membranes was analyzed by energy dispersive X-ray spectroscopy (EDX), which was an auxiliary equipment of scanning electron microscopy (SEM).

Fourier-transform infrared spectroscopy

Fourier-transform infrared (FT-IR) spectra were recorded between 4,000 and 400 cm^{-1} by a Nicolet 5700 Fourier transform infrared spectrometer (Thermo Electron). About

200 mg of IR spectroscopic-grade KBr pellets was used with 1 mg of the polymer samples.

X-ray diffraction

X-ray diffraction (XRD) was used to identify the crystalline materials of the membranes with a diffractometer (Bruker D8 Advance) using a solid detector and Cu Kα radiation at 40 kV and 40 mA. The 2θ ranges were from 2° to 60°.

Thermal gravimetric analysis

Thermal gravimetric analysis (TGA) was used to analyze the thermal stability of the composite membranes. Thermo gravimetric analysis was carried out using a thermogravimetric analyser (Netsch STA-409) from 30 to 900 °C at a rate of 10 °C/min under normal atmospheric pressure (flow rate, 30 ml/min).

Water uptake and swelling ratio

The swelling behavior of the membranes produced was studied by measuring their water uptake and swelling ratio. The membrane samples were dried at 60 °C for 48 h. The weighed films were soaked in deionised water overnight for different times at determined temperatures. The water uptake and the swelling ratio were calculated as follows:

$$\text{Water uptake}(\%) = \frac{\omega_w - \omega_d}{\omega_d} \times 100\%$$

where ω_w and ω_d are the weight of the wet and dry membranes, respectively.

$$\text{Swelling ratio}(\%) = \frac{L_w - L_d}{L_d} \times 100\%$$

where L_w and L_d are the thickness of the wet and the dry membranes, respectively.

Oxidative stability

The oxidative stability of composite membranes was investigated by observing the degradation behavior of membranes when they were immersed in 25 mL Fenton's reagent (30 ppm $FeSO_4$ in 30 % H_2O_2) at room temperature. The membrane was first weighed (O_1) and then immersed in Fenton's reagent for 3 h. It was then washed with deionized water and dried in a vacuum at 10 °C for 24 h, after which the membrane was weighed quickly (O_2). The oxidative stability of composite membranes was calculated using the equation:

$$OS = \frac{O_1 - O_2}{O_1} \times 100\%$$

Mechanical properties

The tensile strength of the blend membranes were measured at room temperature using a tensile testing machine (CMT6203, China) at a crosshead speed of 2 mm/min. The width of the sample was b (millimeters) and the thickness of the composite membrane was d (millimeters). The maximum load was recorded as P (N). All the measurements were performed at 25±2 % RH. The tensile strength (δt) of the composite membrane can be calculated using Eq. (4):

$$\delta t = \frac{P}{bd}$$

Proton conductivity

The proton conductivities of the membranes were calculated from AC impedance spectroscopy data using a Potentiostat Model 263A workstation (Perkin-Elmer Instruments) with a lock-in amplifier (Model 5210, 1 Hz–10 kHz; Perkin-Elmer Instruments). The software Powersuite was used to collect the data and plot the figures. The samples of the membranes were fully humidified by water vapor at all temperatures.

Methanol permeability

Methanol permeabilities of the samples were measured using a diffusion cell constructed in our laboratory following the design described in literature [28]. The diffusion cell consisted of two compartments that were separated by a vertical membrane. One compartment of the cell was filled with 1 mol/L methanol solution while the other compartment was filled with deionized water. The compartments were stirred continuously during permeability measurements. The methanol concentration in the water compartment was determined using gas chromatography. The methanol permeability (P, square centimeters per second) was calculated from the equation:

$$P = \frac{SV_BL}{AC_{A0}}$$

where S is the slope of the curve of methanol concentration versus time in the water compartment, V_B (milliliters) is the volume of the water compartment,

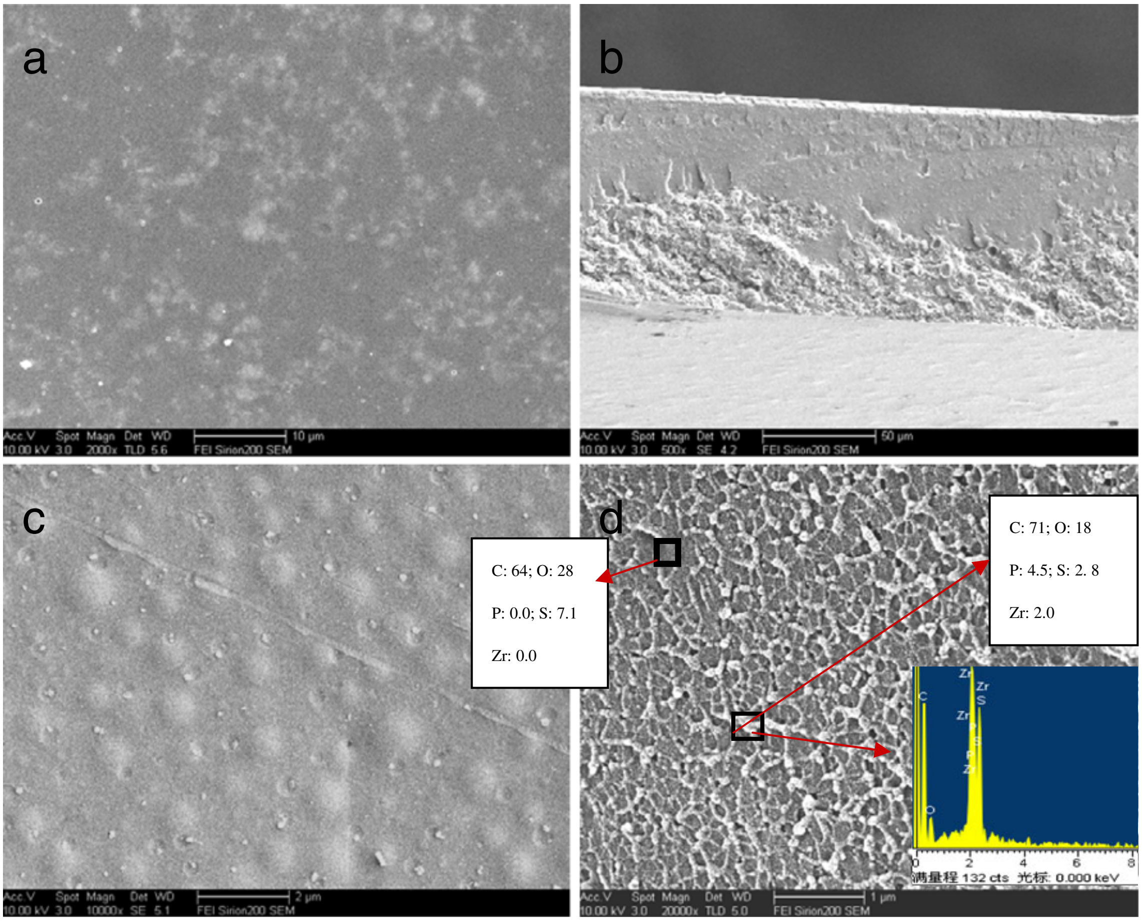

Fig. 1 SEM and EDS of SPPES/ZrSPP composite membranes **a** surface of 10 wt% membrane, **b** cross-section of 10 wt% membrane, **c** surface of 30 wt% membrane, **d** cross-section of 30 wt% membrane

C_{A0} (moles per liter) is the initial concentration of methanol in the methanol compartment, and L (centimeters) and A (square centimeters) are the thickness and area of the membrane, respectively.

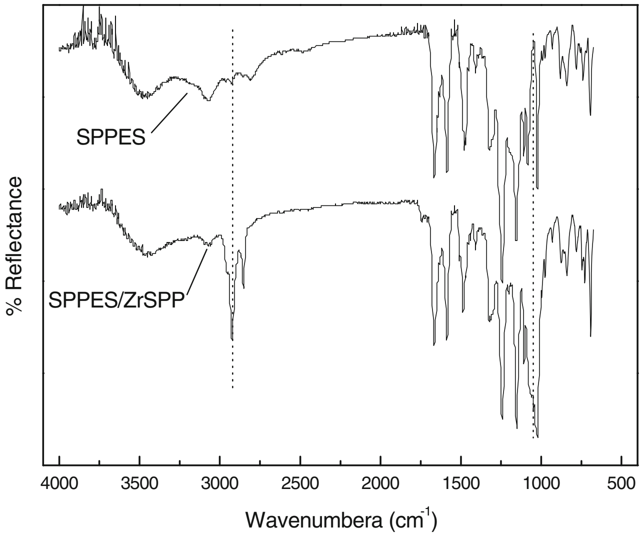

Fig. 2 FT-IR of SPPES membrane and SPPES/ZrSPP membrane

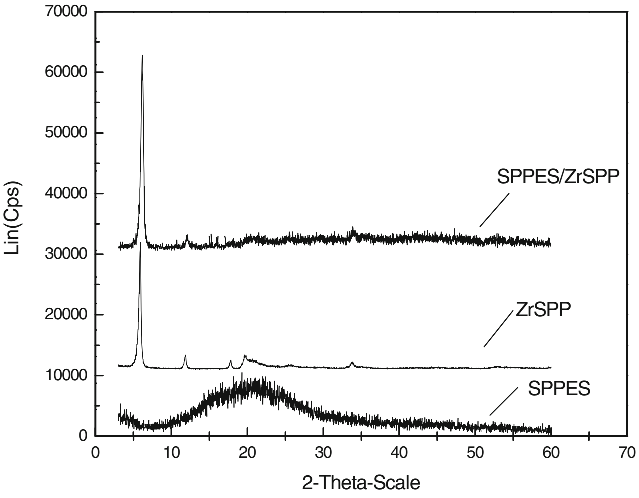

Fig. 3 XRD of ZrSPP, SPPES membrane, and SPPES/ZrSPP composite membrane

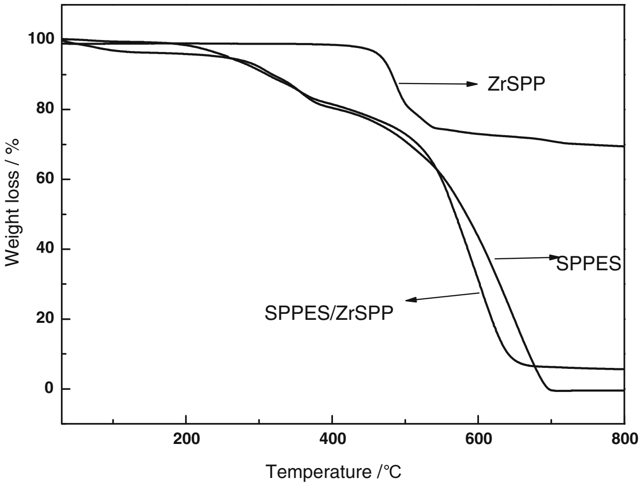

Fig. 4 TG of ZrSPP, SPPES, and SPPES/ZrSPP membrane

Results and discussion

SEM and EDX

The morphology of the composite membrane samples was observed by SEM. The surface and fracture surface SEM images of the 10 wt% composite membranes are shown in Fig. 1a and b show that there is a homogenous dispersion of ZrSPP into the membranes. Fracture surfaces have a dense structure. The surface of SPPES/ZrSPP (30 wt%) composite membrane (Fig. 1c) is mainly smooth and dense. There are a small number of ZrSPP particles well dispersed on the surface. From the EDX of fracture surface of SPPES/ZrSPP (30 wt%) membrane (Fig. 1d), we can see that the hatched section is SPPES, the white section is ZrSPP. ZrSPP form a lattice structure, SPPES tightly wrapped ZrSPP skeleton structure, that is quite dense.

FT-IR spectroscopy

The FT-IR spectra of the SPPES and SPPES/ZrSPP composite membranes are shown in Fig. 2. Most FT-IR absorption did not change after ZrSPP doping into the SPPES membrane. The broad and strong absorption at 3,480 cm^{-1} is attributed to the stretching of –OH in $–SO_3H$ [17]. Peaks at 1,326 and 1,151 cm^{-1} are assigned to asymmetrical and symmetrical stretching of characteristic sulfone [13]. Absorption at 1,025 cm^{-1} is corresponded to the stretching of S=O in $–SO_3H$. However, the peak at 1,060 cm^{-1} in SPPES/ZrSPP composite membrane is characteristic absorption peak of ZrSPP, it is due to the stretching of P–O [29]. In the spectrum of the composite membrane, a new absorption peak can be observed at 2,900 cm^{-1} caused by the hydrogen bonding between sulfonic acid and phosphonic acid [15]. The observation of this peak clearly indicates strong interaction between SPPES and ZrSPP.

XRD

The XRD patterns of the ZrSPP, SPPES, and the SPPES/ZrSPP composite membranes are presented in Fig. 3. From the figure, ZrSPP shows good crystallinity and obvious diffraction peaks at $2\theta=5.9°$, 11.8°, 17.8°, and 19.8°. ZrSPP shows a pattern typical for layered compounds with well pronounced reflections. It shows two distinct reflections of layered structure. The interlayer distance (d) of the XRD pattern is 13–15 Å. The XRD spectra of SPPES/ZrSPP composite membranes also shows crystalline features with sharp peaks at $2\theta=5.9°$. It indicates that the molecule structure of ZrSPP is not destroyed. The diffraction peaks are weak in the composite membrane. This is a consequence of the finely dispersed ZrSPP molecules in the polymer matrix.

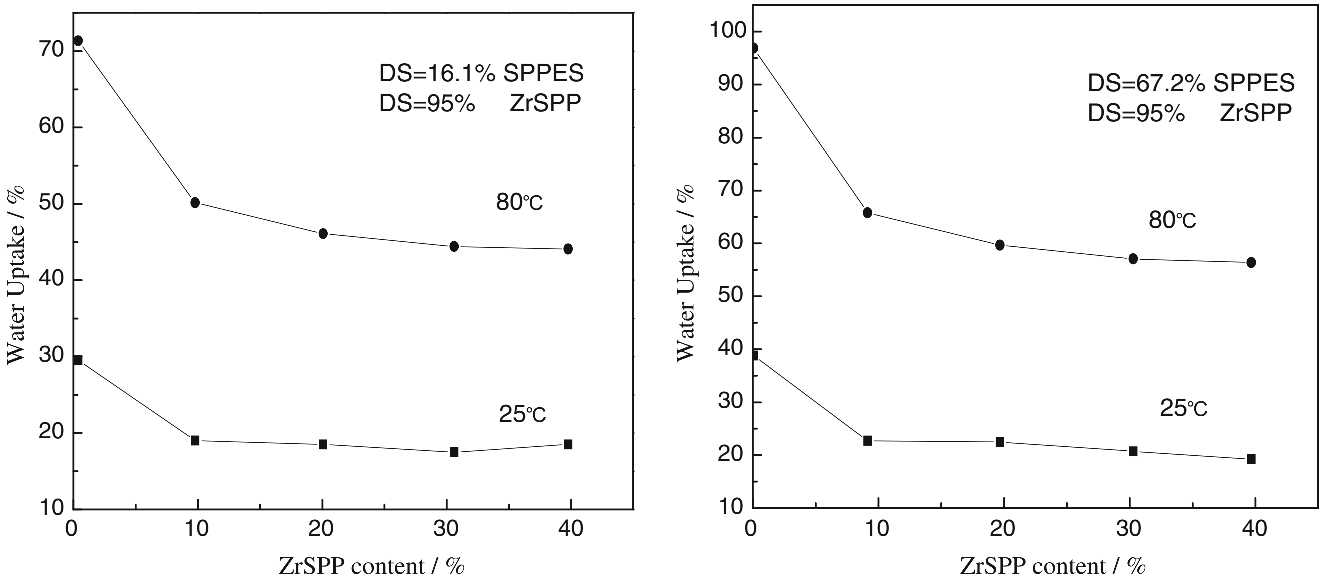

Fig. 5 Water uptake of SPPES membrane and SPPES/ZrSPP composite membranes

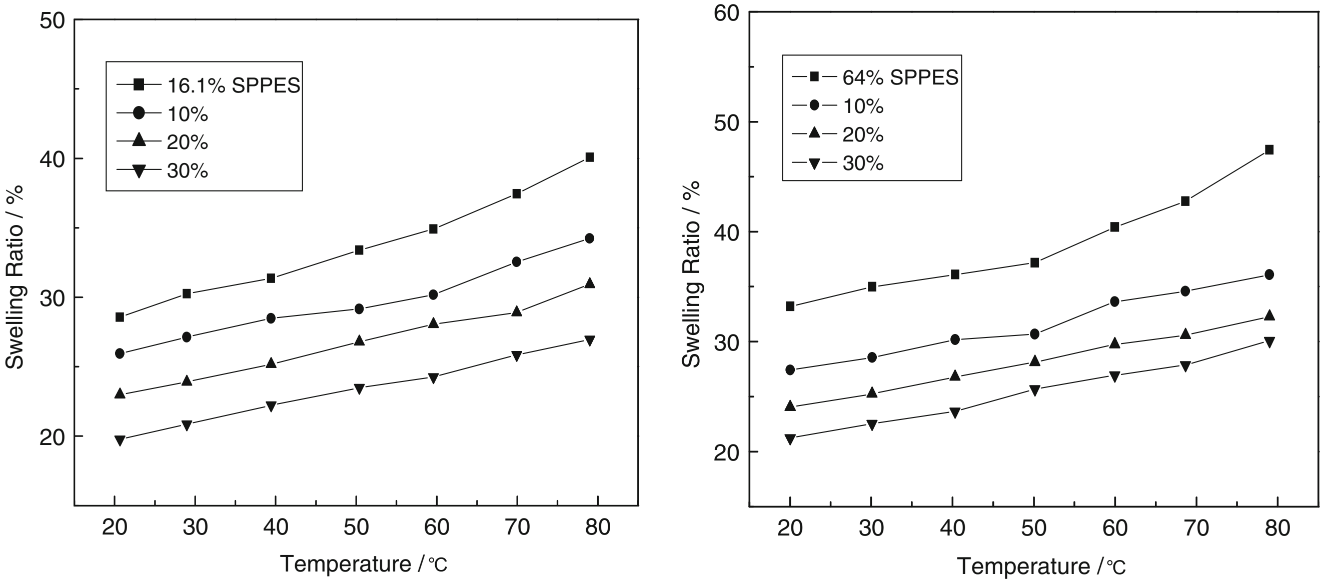

Fig. 6 Swelling ratio of SPPES membrane and SPPES/ZrSPP composite membranes

And the interaction between SPPES and ZrSPP make the composite membrane become more density.

TGA of the SPPES/ZrSPP composite membrane

The thermal stabilities of the ZrSPP, SPPES, and the SPPES/ZrSPP composite membranes were studied by TGA (Fig. 4). The SPPES membrane has a slightly weight loss below 200 °C. This is due to the water loss. ZrSPP has good thermal stability; it has no obvious weight loss below 400 °C. The SPPES/ZrSPP composite membrane has no weight loss below 200 °C, ZrSPP might interact strongly with water molecules and keep water molecules from evaporating. The T>200 °C sulfonic acid groups start to fall off. T>400 °C the main polymer start to degradate. The results indicate that the composite membranes have adequate thermo-stabilities under temperatures below 200 °C.

Water uptake

The water uptake of the SPPES/ZrSPP composite membranes is shown in Fig. 5. At 25 °C, the water uptake of SPPES (DS 16.1 %) membrane is 30 % (pure SPPES) to 17.7 % (SPPES/ZrSPP (30 wt%)), lower than SPPES (DS 64 %) membrane which is 39.1 % (pure SPPES) to 18.7 % (SPPES/ZrSPP (30 wt%)). At 80 °C, the water uptake of SPPES (DS 16.1 %) membrane is 72.3 % (pure SPPES) to 45 % (SPPES/ZrSPP (30 wt%)), also lower than SPPES (DS 67.2 %) membrane which is 96.9 % (pure SPPES) to 58.7 % (SPPES/ZrSPP (30 wt%)). The water uptake of the membranes increases as temperature and DS increase, as hydrophilic groups, the more sulphated groups, and the stronger hydrophilic force. The water uptake decreases with an increase in ZrSPP content. At low temperature, ZrSPP have small effect on water uptake of composite membranes.

Swelling ratio

The swelling ratio of the SPPES/ZrSPP composite membranes is shown in Fig. 6. The swelling ratio of the membranes increases as DS and temperature increases. But it decreases with an increase in ZrSPP content. At 20 °C, ZrSPP reduce swelling ratio just from 28.1 % (pure SPPES (DS 16.1 %) membrane) to 19.7 % (SPPES (DS 16.1 %)/ZrSPP (30 wt%) composite membrane). However, ZrSPP greatly reduce swelling ratio of composite membranes at higher temperature. At 80 °C, it reduce swelling ratio from 39.7 % (pure SPPES (DS 16.1 %) membrane) to 25 % (SPPES (DS 16.1 %)/ZrSPP (30 wt%) composite membrane). The swelling ratio of SPPES

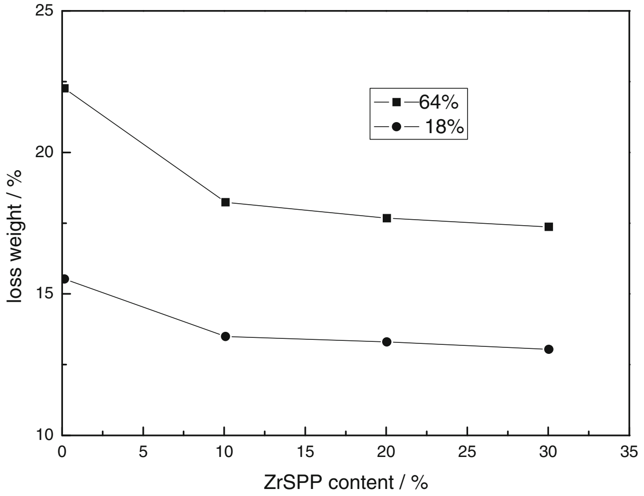

Fig. 7 Oxidative stability of SPPES/ZrSPP composite membranes

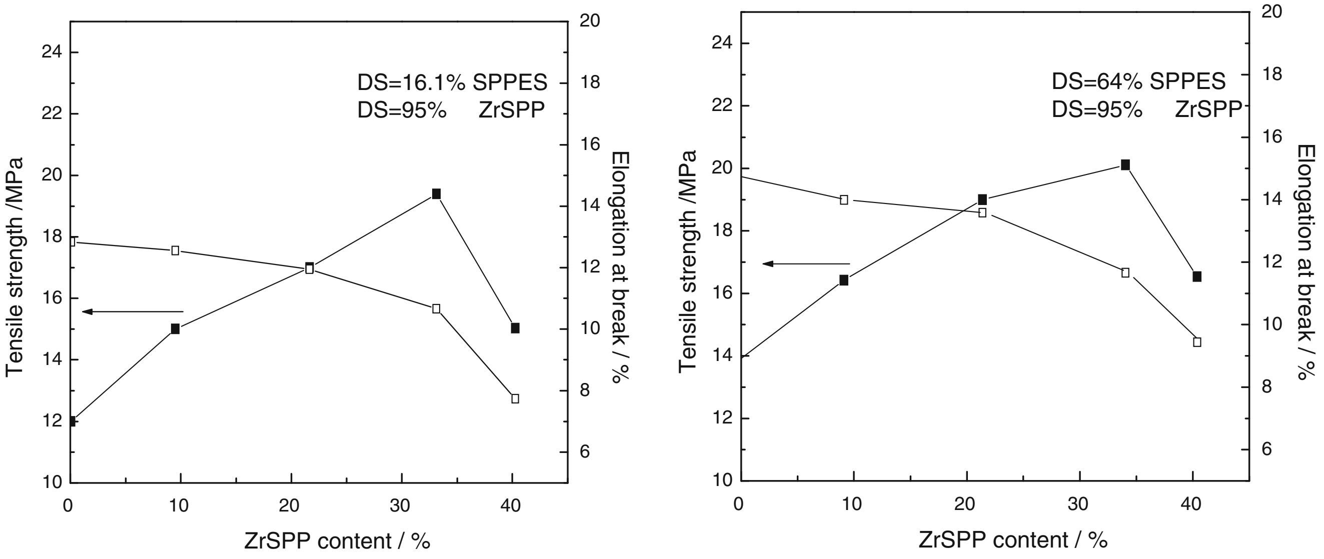

Fig. 8 Tensile strength and elongation at break of SPPES membrane and SPPES/ZrSPP composite membrane

(DS 64 %) membranes are from 32.1 % (pure SPPES) to 20.9 % (SPPES/ZrSPP (30 wt%)) at 20 °C, and 47.5–26 % at 80 °C. And SPPES (DS 16.1 %) membrane is from 32.1 % (pure SPPES) to 20.9 % (SPPES/ZrSPP (30 wt%)). The formation of intermolecular hydrogen bonds between ZrSPP and SPPES and the ZrSPP lattice structure greatly restricts the swelling of the membranes. ZrSPP enhances the dimensional stability of the membranes in wet/dry condition.

Oxidative stability

The Fenton solution test was carried out to reveal the relationship between the addition of ZrSPP and the oxidation-resistant properties of the composite membrane. The results can be seen in Fig. 7. Oxidative stability decreases as DS increase. Weight loss decreases from 22 % of pure SPPES (DS 64 %) to 18 % of SPPES (DS 64 %)/ZrSPP (10 wt%), 15.3 % of SPPES (DS 18 %) to 13.8 % of SPPES (DS 18 %)/ZrSPP (10 wt%). The addition of ZrSPP greatly reduces weight loss after the membrane has been oxidized, showing good resistance to strong oxidization.

Mechanical strength of membranes

The tensile strength of SPPES/ZrSPP composite membranes is illustrated in Fig. 8. The tensile strength of SPPES (DS 16.1 %) membrane is 12.2 MPa; SPPES (DS 64 %) membrane is 13.8 MPa. This property of membranes with two different DS appeared to be very

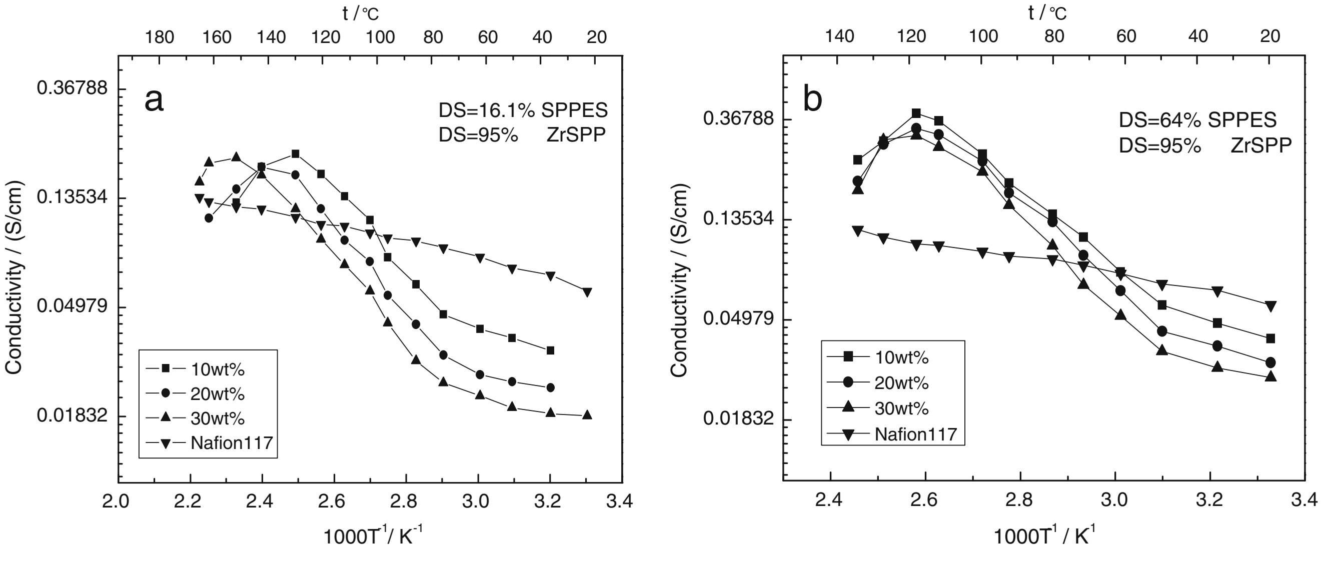

Fig. 9 Proton conductivity of Nafion 117 and SPPES/ZrSPP composite membranes

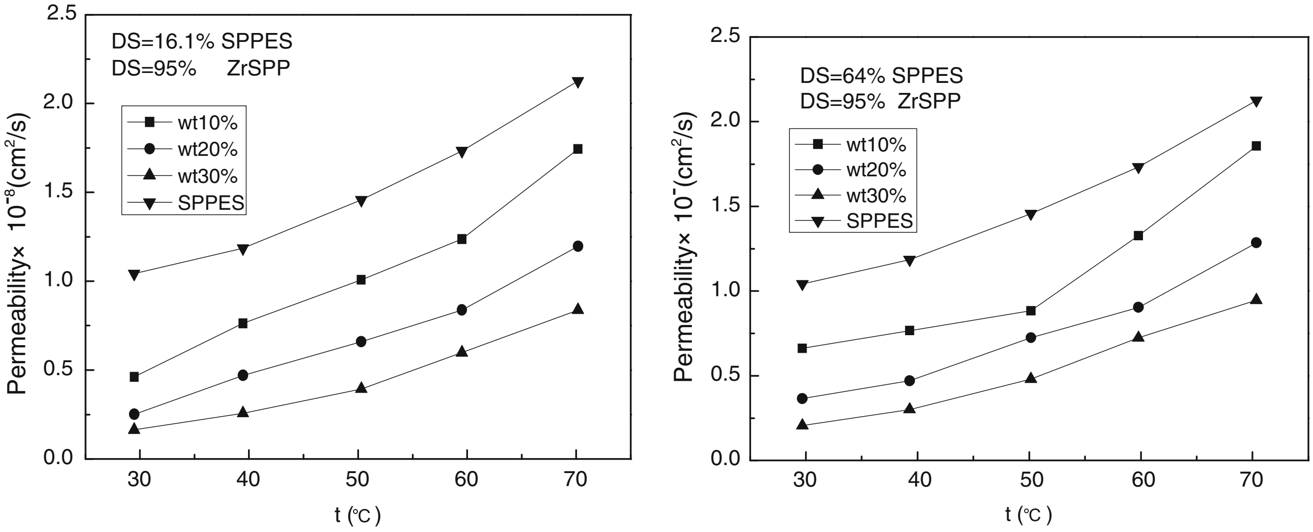

Fig. 10 Methanol permeability of SPPES membrane and SPPES/ZrSPP composite membranes

sensitive to the ZrSPP content, as the tensile strength increased rapidly with increases in ZrSPP content. SPPES (DS 16.1 %) membrane/ZrSPP (30 wt%) is 19.5 MPa; SPPES (DS 64 %) membrane/ZrSPP (30 wt%) is 20 MPa. This behavior could be attributed to the ZrSPP nanoparticles that were uniformly dispersed throughout the polymer and formed a lattice structure. SPPES and ZrSPP have a good compatibility, formed intense intermolecular forces, SPPES combined firmly around the ZrSPP lattice structure. As more ZrSPP incorporated into SPPES polymers, the tensile strength decreased. The reason could be that the introduction of ZrSPP into the sulfonated polymer damaged the ordering of the aggregative state. As a result, the composite membranes lost their original flexibility due to the rigidity of ZrSPP.

Proton conductivity

Conductivity is an important parameter for PEM. There are two principal mechanisms of proton transfer: one is “Grotthuss”, protons hop from one hydrolyzed ionic site ($SO^{3-}H_3O^+$) to another across the membrane. The other is “Vehicle” mechanism. In “Vehicle” mechanism, the water connected protons ($H^+(H_2O)_X$) in the result of the electroosmotic drag carry the one or more molecules of water through the membrane and itself are transferred with them to finish proton transfer [30]. For SPPES/CeSPP composite membrane “Grotthuss” mechanism plays a leading rule on proton transfer, and “Vehicle” mechanism played a relatively minor role. Hydrogen bonds between SPPES and CeSPP also facilitate proton transfer.

The conductivity of ZrSPP at room temperature is about 10^{-2} S/cm. The proton conductivities of Nafion®117 and SPPES/ZrSPP composite membranes with different ZrSPP contents are presented in Fig. 9. Proton conductivities of SPPES/ZrSPP composite membranes increase with DS and decrease with increasing ZrSPP content. As shown in Fig. 9a, the SPPES (DS 16.1 %)/ZrSPP (10 wt%) composite membrane has conductivity similar to Nafion®117 at 100 °C and reaches 0.18 S/cm at 130 °C. The conductivity of the 30 wt% composite membrane reaches 0.18 S/cm, but 150 °C. ZrSPP enhance the thermal stability of composite membranes. It makes the composite membrane maintain excellent proton conductivity at high temperature. In Fig. 9b, the SPPES (DS 64 %)/ZrSPP (10 wt%) composite membrane has similar conductivity to Nafion®117 at 60 °C and reach 0.39 S/cm at 120 °C, almost three times higher than that of Nafion®117.

The dependence of a membrane’s conductivity on temperature can be expressed by the Arrhenius relationship:

$$\sigma = A \exp\left(-\frac{E_{\text{act}}}{\text{RT}}\right)$$

where σ, A, Ea, R, and T denote proton conductivity, frequency factor, activation energy for proton conduction, gas constant, and absolute temperature, respectively.

For the SPPES membrane, E_{act}=26.24 kJ/mol. That of SPPES/ZrSPP composite membranes with different DS and ZrSPP content is 17.76 kJmol^{-1}. Ion mobility (u) increases with the temperature. High E_{act} suggests that the temperature significantly influenced the ion mobility. The Eact of SPPES/ZrSPP composite membrane is higher than Nafion117 (6.81 kJ/mol), when the temperatures increase, the ion mobility of composite membrane increased more visibly than Nafion117.

Methanol permeability

The methanol permeabilities of SPPES/ZrSPP composite membranes at different temperatures are shown in Fig. 10. The methanol permeabilities of composite membranes increase with temperature and decrease with increased ZrSPP content. In addition, the methanol permeabilities of SPPES/ZrSPP composite membranes are lower than those in pure SPPES. In composite membranes, ZrSPP are an excellent alcohol barrier, which can disturb the molecular channels of methanol and increase the membrane's resistance to methanol permeability. All the SPPES/ZrSPP composite membranes reveal methanol permeabilities in the range of 2.1×10^{-8} to $0.13\times10^{-8}\,\mathrm{cm^2/s}$, a considerable reduction compared with Nafion®117($10^{-6}\,\mathrm{cm^2/s}$).

Conclusions

The SPPES/ZrSPP composite membranes were prepared by ZrSPP doping to SPPES in DMAc. The FT-IR, SEM, EDX, and XRD results show that ZrSPP shows good dispersibility in SPPES, and strong hydrogen bonds formed between them. ZrSPP form a lattice structure in the composite membrane. Water uptakes of composite membrane are reduced, dimensional stability of the membranes in wet/dry condition become stronger. The composite membranes exhibit high thermal stability and excellent proton conductivities. The proton conductivity of the SPPES (DS 16.1 %)/ZrSPP (30 wt%) composite membrane is 0.18 S/cm at 150 °C, SPPES (DS 64 %)/ZrSPP (10 wt%) composite membrane has a conductivity reached 0.39 S/cm at 120 °C, which is three times more than that of the Nafion® 117 membrane. These results show that SPPES/ZrSPP composite membranes have a promising future for application in direct methanol fuel cells working at medium temperatures. The SPPES/ZrSPP composite membranes have low methanol permeabilities, ZrSPP improve barrier properties of SPPES membrane.

Acknowledgments This work was financially supported by the National Natural Science Foundation of China (grant nos. 21076119, 21276148, and 20776081) and the Natural Science Foundation of Shandong Province, China (grant no. ZR2010BM004 and Y2006B37).

References

1. Wang YJ, Wilkinson DP, Zhang JJ (2011) Noncarbon support materials for polymer electrolyte membrane fuel cell electrocatalysts. Chem Rev 111:7625–7651
2. Dixon D, Wippermann K, Mergel J, Schoekel A, Zils S, Roth C (2011) Degradation effects at the methanol inlet, outlet and center region of a stack MEA operated in DMFC. J Power Sources 196:5538–5545
3. Nachiappan N, Paruthimal Kalaignan G, Sasikumar G (2012) Novel synthesis and characterization of nanocomposite Pt-WO3-TiO2/C electrocatalyst for PEMFC. Ionics. doi:10.1007/s11581-012-0709-9
4. Wang CY, Li NW, Shin DW, Lee SY, Kang NR, Lee YM, Guiver MD (2011) Fluorene-based poly(arylene ether sulfone)s containing clustered flexible pendant sulfonic acids as proton exchange membranes. Macromolecules 44:7296–7306
5. Fu LC, Xiao GY, Yan DY (2010) Synthesis and characterization of sulfonated poly(arylene ether ketone/ketone phosphine oxide)s as proton exchange membranes. J Membr Sci 362:509–516
6. Liu D, Liao HY, Tan N, Xiao GY, Yan DY (2011) Sulfonated poly (arylene thioether phosphine oxide)/sulfonated benzimidazole blends for proton exchange membranes. J Membr Sci 372:125–133
7. Tan N, Xiao GY, Yan DY, Sun GM (2010) Preparation and properties of polybenzimidazoles with sulfophenylsulfonyl pendant groups for proton exchange membranes. J Membr Sci 353:51–59
8. DeLuca NW, Elabd YA (2006) Polymer electrolyte membranes for the direct methanol fuel cell: a review. J Polym Sci Part B Polym Phys 44:2201–2225
9. Nachiappan N, Paruthimal Kalaignan G, Sasikumar G (2012) Effect of nitrogen and carbon dioxide as fuel impurities on PEM fuel cell performances. Ionics. doi:10.1007/s11581-012-0730-z
10. Geormezi M, Deimede V, Kallitsis JK, Neophytides S (2012) Polymer blends based on copolymers bearing both side and main chain pyridine units as proton exchange membranes for high temperature fuel cells. J Membr Sci 396:57–66
11. Jun Y, Zarrin H, Fowler M, Chen ZW (2011) Functionalized titania nanotube composite membranes for high temperature proton exchange membrane fuel cells. Int J Hydrogen Energy 36:6073–6081
12. Jaafar J, Ismail AF, Matsuura T, Nagai K (2011) Performance of SPEEK based polymer–nanoclay inorganic membrane for DMFC. J Membr Sci 382:202–211
13. Gao Y, Robertson GP, Guiver MD, Jian XG, Mikhailenko SD, Wang K, Kaliaguine S (2003) Sulfonation of poly(phthalazinones) with fuming sulfuric acid mixtures for proton exchange membrane materials. J Membr Sci 227:39–50
14. Zhao S, Wang P, Wang C, Sun X, Zhang L (2012) Thermostable PPESK/TiO2 nanocomposite ultrafiltration membrane for high temperature condensed water treatment. Desalination 299:35–43
15. Li ZF, Dong FL, Xu LJ, Wang SW, Yu XJ (2010) Preparation and properties of medium temperature membranes based on zirconium sulfophenylphosphate/sulfonated poly(phthalazinone ether sulfone ketone) for direct methanol fuel cells. J Membr Sci 351:50–57
16. Dong FL, Li ZF, Wang SW, Xu LJ, Yu XJ (2011) Preparation and properties of sulfonated poly(phthalazinone ether sulfone ketone)/zirconium sulfophenylphosphate/PTFE composite membranes. Int J Hydrogen Energy 36:3681–3687
17. Fang J, Shen PK, Liu QL (2007) Low methanol permeable sulfonated poly(phthalazinone ether sulfone) membranes for DMFCs. J Membr Sci 293:94–99
18. Zhang HW, Shen PK (2012) Recent development of polymer electrolyte membranes for fuel cells. Chem Rev 112:2780–2832
19. Kim TK, Kang M, Choi YS, Kim HK, Lee W, Chang H, Seung D (2007) Preparation of Nafion-sulfonated clay nanocomposite membrane for direct menthol fuel cells via a film coating process. J Power Sources 165:1–8
20. Chang JH, Park JH, Park GG, Kim CS, Park OO (2003) Proton-conducting composite membranes derived from sulfonated hydrocarbon and inorganic materials. J Power Sources 124:18–25
21. Chen CC, Tsi HY, Tsen WC, Chuang FS, Jang SC, Shu YC, Wen S, Gong C (2012) PWA/silica doped sulfonated poly(ether sulfone) composite membranes for direct methanol fuel cells. J Appl Polym Sci 123:1184–1192

22. Lu S, Wang D, Jiang SP, Xiang Y, Lu JZ (2010) HPW/MCM-41 phosphotungstic acid/mesoporous silica composites as novel proton-exchange membranes for elevated-temperature fuel cells. Adv Mater 22:971–976
23. Jalani NH, Dunn K, Datta R (2005) Synthesis and characterization of Nafion®−MO_2 (M=Zr, Si, Ti) nanocomposite membranes for higher temperature PEM fuel cells. Electrochim Acta 51:553–560
24. Zhang ZH, Désilets F, Felice V, Mecheri B, Licoccia S, Tavares AC (2011) On the proton conductivity of Nafion–faujasite composite membranes for low temperature direct methanol fuel cells. J Power Sources 196:9176–9187
25. Yang J, Shen PK, Varcoe J, Wei Z (2009) Nafion/polyaniline composite membranes specifically designed to allow proton exchange membrane fuel cells operation at low humidity. J Power Sources 189:1016–1019
26. Amirinejad M, Madaeni SS, Rafiee E, Amirinejad S (2011) Cesium hydrogen salt of heteropolyacids/Nafion nanocomposite membranes for proton exchange membrane fuel cells. J Membr Sci 377:89–98
27. Krishnan P, Park JS, Yang TH, Lee WY, Kim CS (2006) Sulfonated poly(ether etherketone)-based composite membrane for polymer electrolyte membrane fuel cells. J Power Sources 163:2–8
28. Carretta N, Tricoli V, Picchioni F (2000) Ionomeric membranes based on partially sulfonated poly(styrene): synthesis, proton conduction and methanol permeation. J Membr Sci 166:189–197
29. Dong FL, Li ZF, Wang SW, Wang ZH (2011) Cerium sulfophenyl phosphate, a novel inorgano–organic solid proton-conducting material. Mater Lett 65:1431–1433
30. Park CH, Lee CH, Guiver MD, Lee YM (2011) Sulfonated hydrocarbon membranes for medium-temperature and low-humidity proton exchange membrane fuel cells (PEMFCs). Prog Polym Sci 36:1443–1498